Stabilization of Th^{3+} ions into mixed-valence thorium fluoride

Marc Dubois [a,c,*], Belto Dieudonné [a,c], Adel Mesbah [a,c], Pierre Bonnet [a,c], Malika El-Ghozzi [a,c], Guillaume Renaudin [b,c], Daniel Avignant [a,c]

[a] Clermont Université, Université Blaise Pascal, Laboratoire des Matériaux Inorganiques, BP 10448, F-63000 Clermont-Ferrand, France
[b] Clermont Université, ENSCCF, Laboratoire des Matériaux Inorganiques, BP 10448, F-63000 Clermont-Ferrand, France
[c] CNRS, UMR 6002, LMI, F-63177 Aubière, France

ARTICLE INFO

ABSTRACT

The unusual oxidation state +3 of the thorium has been stabilized into a lithium containing non-stoichiometric mixed-valence (III/IV) thorium fluorinated phase with formula $Li_{2+x}Th_{12}F_{50}$ ($0 < x < 1.8$). This phase is closely related to the $Li_{5.5}Ce_{12}F_{50}$ one, the structure of which has been determined from the combined single-crystal X-ray diffraction and high resolution synchrotron powder diffraction. In these phases, the Li^+ ions can be divided into two groups and are located either in locked positions or in open channels of the three dimensional framework. The amount of Li^+ ions in open channels can be variable, so that the afore mentioned single phase may be considered as an insertion compound. The Li^+ insertion is accompanied by the simultaneous reduction of a part of the Th^{4+} ions, resulting in a mixed-valence III/IV thorium fluoride. The electrochemical insertion of Li^+ ions into the open channels of the host matrix has been carried out at 60 °C, using an alkylcarbonate PC–$LiClO_4$ 1 M electrolyte. The Li^+ and Th^{3+} contents, both in the starting composition and the Li^+ inserted ones, were investigated by high resolution solid state ^7Li NMR and EPR, respectively.

© 2010 Elsevier Inc. All rights reserved.

1. Introduction

The presence of thorium in the +3 oxidation state is very unusual in the solid state, where Th^{4+} is the stable ion [1,2]. Nevertheless, thorium triiodide (ThI_3) has been formed either by heating the metal with the stoichiometric amount of iodine in vacuum at 550 °C or by reduction of ThI_4 with appropriate amounts of thorium metal. The resulting compound reacts with water with the evolution of H_2 and formation of Th^{4+}. The reduction of a ThF_4/ThO_2 mixture with thorium metal at 1200–1500 °C results in ThOF [2,3]. Those drastic experimental conditions to obtain Th^{3+} highlight the non-stability of this ion in the solid state. In the present paper, we focus on thorium fluoride in order to investigate the stabilization of Th^{3+} in a Th^{3+}/Th^{4+} mixed-valence compound. Among the numerous studies devoted to lanthanide and actinide fluorides, data on mixed-valence compounds were less reported in the literature [4–17].

Recently, the structure of the first mixed-valence cerium fluoride with stoichiometry $Li_{5.5}Ce_{12}F_{50}$ has been successfully solved, refined and described by combining single-crystal X-ray diffraction and high resolution synchrotron powder diffraction data [18,19]. The initial stoichiometry "$LiCe_4F_{17}$" [20–23] has been corrected to $Li_{5.5}Ce_{12}F_{50}$ using X-ray diffraction, ^7Li nuclear magnetic resonance (NMR) and X-ray photoelectron spectroscopy (XPS) data. In the present paper, this study is extended to the LiF–MF_4 (M=Ce and Th) binary systems. These compounds have been initially formulated as LiM_4F_{17} [20–23], but the structural characterizations [22,23] underline an ambiguity about their real stoichiometry. In a first step, X-ray diffraction data of thorium and cerium compounds will be investigated to underline their isostructural feature. ^1H and ^7Li nuclear magnetic resonance will be then discussed to explain the different compositions successively reported in the literature for the same compounds, i.e. "$LiTh_4F_{17}$" and $Th_6F_{24} \cdot H_2O$ [22,23].

The crystal structure of $Li_{5.5}Ce_{12}F_{50}$ is related to the structure of CeF_4 [18], with the presence of lithium cations allowed by an opened channel network. One part of Li^+ is locked and the other part is relatively free to move along the channels network. The insertion of Li^+ into the channel leads to the reduction of one equivalent part of Ce^{4+}–Ce^{3+}. In other words, this fluoride can be described as an insertion compound. An explicit formula of the compound has been proposed as $Li_{2+x}Ce_x^{3+}Ce_{12-x}^{4+}F_{50}$, indicating the minimum amount of lithium (2 per unit formulae) and the progressive reduction of cerium (from Ce^{4+} to Ce^{3+}) when inserting the x supplementary lithium cations. Considering the isostructural behaviour of cerium and thorium mixed-valence fluorides, the electrochemical insertion of lithium ions was investigated in order to change the Th^{3+}/Th^{4+} ratio in the $Li_{2+x}Th_x^{3+}Th_{12-x}^{4+}F_{50}$ thorium

* Corresponding author at: Clermont Université, Université Blaise Pascal, Laboratoire des Matériaux Inorganiques, BP 10448, F-63000 Clermont-Ferrand, France. Fax: +33 4 73 40 71 08.
E-mail address: marc.dubois@univ-bpclermont.fr (M. Dubois).

fluoride. In the present work, in addition to the synthesis of Th^{3+}/Th^{4+} mixed-valence, the electrochemical process also allows the control of the Th^{3+}/Th^{4+} ratio contrary to the solid state synthesis.

2. Experimental

2.1. Synthesis

Samples were synthesized by solid state reaction involving mixture of LiF and ThF_4 starting materials in the 1/4 molar ratio. Pure ThF_4 thorium tetrafluoride has been prepared by the following route: (i) dissolution of $Th(NO_3)_4$ in HF solution (40%) and (ii) after evaporation of the solution, drying of the resulting powder; this one was fluorinated under pure F_2 gas stream at 500 °C. LiF (99.9%, Aldrich) was dehydrated by heating at 110 °C overnight in primary vacuum.

The 1/4 mixture was introduced and heated in platinum tubes (40 mm of length, 5 mm of diameter) further sealed under dry argon atmosphere. The airtight platinum capsule was heated at 300 °C for 24 h, and then a temperature of 550 °C was applied during 72 h.

In order to investigate the possible exchange between Li^+ ions and H_2O molecules with change of the oxidation state of thorium, the as-synthesized sample was treated in boiling water for 2 h under magnetic stirring, and then dried under primary vacuum for 12 h at 120 °C.

2.2. Characterization

2.2.1. X-ray powder diffraction (XRPD)

X-ray powder diffraction (XRPD) patterns were recorded on a X'Pert Pro Philips diffractometer, with $\theta-\theta$ geometry, equipped with a solid detector X-Celerator, a graphite back-end monochromator, and using Cu $K\alpha$ radiation ($\lambda=1.54184$ Å). PXRD patterns were recorded at room temperature in the interval $3° < 2\theta < 120°$, with a step size $\Delta 2\theta=0.0167°$ and a counting time of 200 s per step. A total counting time of 3.5 h was used. PXRD patterns were refined by the Rietveld method with the FullProf.2k program [24] using (as initial parameters) the structural parameters previously determined for $Li_{5.5}Ce_{12}F_{50}$ [18,19].

2.2.2. ^7Li and ^1H MAS NMR

The ^7Li and ^1H NMR spectra were recorded with magic angle spinning (MAS) at room temperature, using a Bruker AVANCE 300 spectrometer, operating at the frequencies of 116.6 and 300.1 MHz for ^7Li and ^1H nuclei, respectively. Spinning rate was equal to 14 kHz using a 4 mm Bruker probe. A single $\pi/2$ pulse sequence was used (τ-acquisition with $\tau=6$ and 5 µs for ^7Li and ^1H nuclei, respectively). Of about 1000 and 128 scans were recorded with a recycling time of 1 and 5 s for ^7Li and ^1H, respectively. The ^1H chemical shift refers to tetramethylsilane (TMS) by using adamantane as an external reference. The ^7Li chemical shifts are given with respect to solid LiCl.

2.2.3. EPR spectroscopy

EPR spectra were recorded at room temperature, using an X Band Bruker EMX spectrometer operating at 9.653 GHz. Diphenylpicrylhydrazyl was used to calibrate the resonance frequency $g=2.0036 \pm 0.0002$. Mixed-valence thorium fluorides were characterized by the EPR spectroscopy in the initial state and after a complete reduction. This sample was prior dried under dynamic vacuum, ground and set into a glass tube of 0.5 mm in diameter; the preparation of the samples was carried out in a glove box under an inert atmosphere (argon).

2.3. Electrochemical insertion of Li^+

Electrochemical measurements were carried out using a conventional two electrodes cell (Swagelok), where lithium was used both as reference and counter electrode. Then, the potentials refer to a $Li^+/Li°$ electrode. The working electrode was formed by thorium fluoride ($Li_{2+x}Th_{12}F_{50}$) (about 80% by weight (w/w)), carbon black (CB, 10%, w/w) to insure electronic conductivity, and polyvinylidene difluoride (PVDF, 10%, w/w) as the binder. The mass of active material was close to 4.0 mg. After stirring in propylene carbonate (PC), this mixture was spread thinly onto a collector by evaporation of PC. Then, it was vacuum dried for 1 h at 150 °C. A PVDF microporous film wetted with $LiClO_4$ dissolved in propylene carbonate (PC 1 mol L^{-1}) was sandwiched between the working electrode and a lithium metal foil. The cells were assembled in an argon-filled glove box. Prior to use $LiClO_4$ (Aldrich, purity 99%) was outgassed under dynamic vacuum at 150 °C and PC was doubly distilled to remove traces of water. Cyclic voltammetry was performed at 60 °C between 4.5 and 1.5 V vs. $Li^+/Li°$ with a linear potential sweeping of 0.17 mV s^{-1}.

3. Results and discussion

3.1. Structural properties

3.1.1. Structural characterization

XRPD analysis of the synthesized sample has indicated that the sample is single phase. The X-ray powder pattern evidences that our synthesized Th-compound is isotypic with $Li_{2+x}Ce_{12}F_{50}$. The $Li_{2+x}Ce_{12}F_{50}$ structure has been recently characterized in details [18,19]. The great similitude between the two powder patterns (showing in Fig. 1A) gives a good indication of the isostructural feature between these two thorium and cerium fluorides. It has been confirmed by Rietveld analysis performed on the $Li_{2+x}Th_{12}F_{50}$ powder pattern (Fig. 1B). Rietveld refinement has been performed by using the Profile Matching procedure. The refinement of the positional parameters (68 independent atomic positions in general $2a$ Wyckoff site; i.e. 204 independent parameters) is inconceivable without using high resolution powder data synchrotron data. Nevertheless, Rietveld refinement results confirm that $Li_{2+x}Th_{12}F_{50}$ phase crystallized with the same monoclinic $P2_1$ symmetry as $Li_{2+x}Ce_{12}F_{50}$ (namely by the perfect difference curve shown in Fig. 1B). Refined lattice parameters for the two phases are gathered in Table 1. The unit cell volume of the thorium phase (1954.10 Å^3) is larger than this of the cerium phase (1790.44 Å^3) in agreement with the larger cationic radius of Th^{4+} compared to Ce^{4+} (1.05 and 0.97 Å in eight-fold coordination [18]). Surprisingly, the b monoclinic axis is smaller in the case of the thorium compound. This smaller b axis could be due to a smaller amount of lithium inserted in the channel network (channels which are quite perpendicular to the b monoclinic axis) associated with a smaller M^{3+}/M^{4+} ratio.

This structural characterization was not able to quantify the lithium amount, or the Th^{3+}/Th^{4+} ratio. Nevertheless, according to the great similitude with the mixed-valence cerium fluoride, the general formulae $Li_{2+x}Th_{12}F_{50}$ (i.e. $Li_{2+x}Th_x^{3+} \cdot Th_{12-x}^{4+}F_{50}$) will be used thereafter; where x is related to the amount of Th^{3+} and Li^+ along the opened channels.

3.1.2. Spectroscopic analyses

Thanks to structural study, which has been carried out on single crystal by Cousson et al. [23], "$LiTh_4F_{17}$" composition, initially reported, has been corrected as $Th_6F_{24} \cdot H_2O$: a hydrated thorium tetrafluoride. Nevertheless, these authors mentioned that the lithium ions are necessary for the synthesis of the hydrated tetrafluoride, although they are absent from the structure. The structure of the
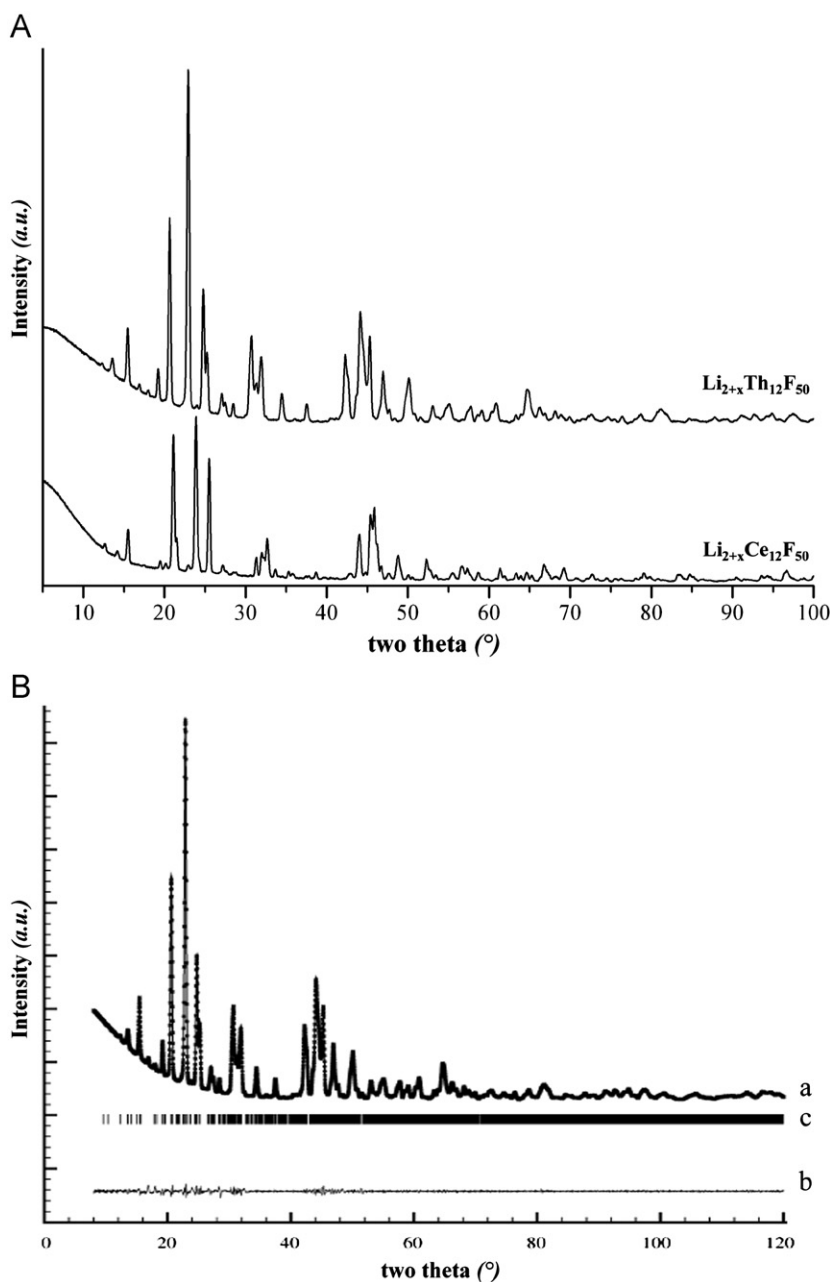
Fig. 1. The XRPD analysis of the $Li_{2+x}Th_{12}F_{50}$ sample: comparison with the X-ray powder pattern of the isotypic $Li_{2+x}Ce_{12}F_{50}$ phase (A), and Rietveld plot of the $Li_{2+x}Th_{12}F_{50}$ phase (B with (a) measured and calculated patterns, (b) difference curve, and (c) Bragg peaks position).

Table 1
Refined lattice parameters for the two isostructural phases with the $P2_1$ symmetry (standard deviations are indicated in parentheses).

Lattice parameters	$Li_{5.5}Ce_{12}F_{50}$ [18,19]	$Li_{2+x}Th_{12}F_{50}$
a (Å)	8.82391(7)	9.2123(1)
b (Å)	22.9188(2)	22.9050(3)
c (Å)	8.85384(7)	9.2610(1)
β (°)	90.6093(2)	90.427(1)
V (Å³)	1790.44(3)	1954.10(5)

$Th_6F_{24} \cdot H_2O$ hydrate compound is related to the $Li_{5.5}M_{12}F_{50}$ structure (M=Th or Ce) with all thorium cations, eight-fold fluorine coordinated (square antiprism), and water molecules occupy a position equivalent to the locked lithium cations into an $Li_{5.5}M_{12}F_{50}$. The single crystals used for this study were obtained by the flux method in (KCl–ZnCl$_2$) chlorides medium and an abundant washing with boiling water was necessary to remove chlorides; the exchange of the lithium ions by water molecules could then occur during washing, taking into account the opened porosities of the structure. This occurred with an oxidation of Th^{3+} into Th^{4+} to conserve the total cationic charges. In order to check this hypothesis, ^1H and ^7Li NMR spectra were recorded using an MAS with 14 kHz spinning rate (Fig. 2a and b, respectively). Two samples were investigated: the as-synthesized fluoride, with supposed $Li_{2+x}Th_{12}F_{50}$ composition, and a sample which was agitated in boiling water during 2 h. First of all, it should be noted that any structural modification was observed by XRD after reaction with water. The total area (normalized by the sample mass) of the ^7Li peaks slightly decreases after water treatment indicating that a few lithium ions are removed (Fig. 2a). A single lorentzian line is not
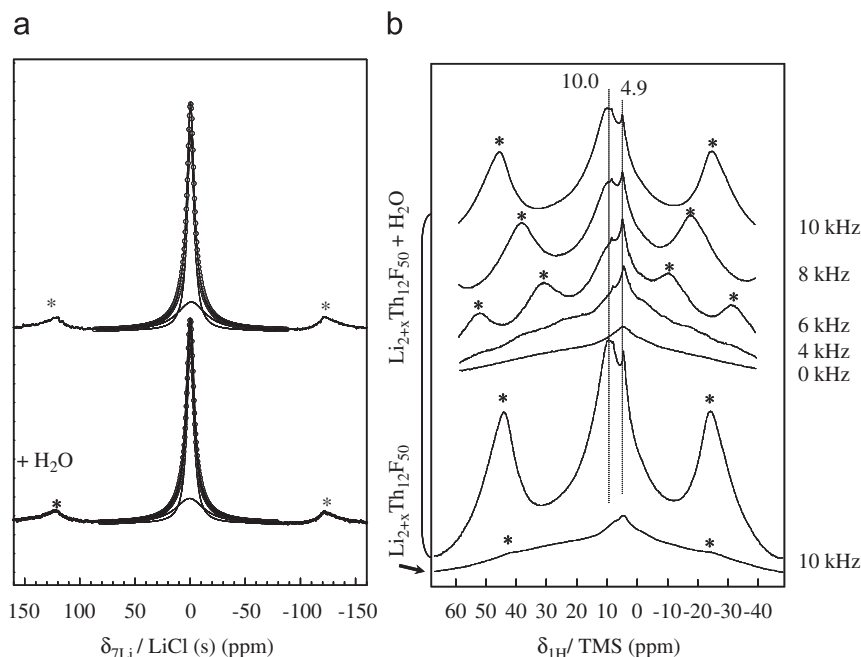
Fig. 2. ^{7}Li (a) and ^{1}H (b) NMR Spectra of $Li_{5.5}Th_{12}F_{50}$ and $Li_{2+x-y}Th_{12}F_{50} \cdot yH_2O$ after water treatment (spinning speed of 14 and 10 kHz, for ^{7}Li and ^{1}H, respectively) and effect of an MAS speed for $Li_{5.5}Th_{12}F_{50}$; * Marks spinning sidebands.

sufficient to fit the spectra. A fitting was then performed with two lorentzian lines at 0 and 1.1 ppm. By analogy with the cerium mixed-valence, lines 1 (at 0 ppm) and 2 (at 1.1 ppm) are assigned to lithium ions in the locked position and along the opened channels, respectively. The S_1/S_2 ratio of the integrated areas change with an increase of 5% after water treatment. A few Li^+ ions have been removed from the channels. Moreover the increase in the Full Width at Half Maximum (FWHM) is noticeable only for the large S_2 line, which is broadened (FWHM increases from 3300 to 3720 Hz) after the water treatment. This indicates that the presence of water molecules in the channels hinders the mobility of the lithium ions. As the changes are weak considering an ^{7}Li NMR, experiments with ^{1}H nuclei have also been carried out. For the as-prepared compound, the content of proton is very weak as revealed by ^{1}H NMR (Fig. 2b). Reaction with water results in a significant increase of the line at 10.0 ppm, which is assigned to water molecules inside the channels. Indeed, an additional weak line is observed at 4.9 ± 0.1 ppm. In order to distinguish between adsorbed and structural H_2O molecules, the spinning rate has been changed and its increase acts only for the ^{1}H nuclei responsible for the line at 10 ppm; the higher the spinning rate, the lower the FWHM. The magic angle spinning, which averages and decreases the ^{1}H–^{1}H homonuclear dipolar coupling and results in the narrowing of the line, is efficient for nuclei located in an ordered neighbouring in crystallized compound. This underlines that these ^{1}H nuclei, with $\delta_{1H} = 10$ ppm, are certainly localized in the open porosity of the hydrated phase $Li_{2+x-y}Th_{12}F_{50} \cdot yH_2O$ and replace a part of the Li^+ ions. The second line at 4.9 ± 0.1 ppm is assigned to adsorbed water molecules. The assumption that the $H_2O \rightarrow Li^+$ exchange, with oxidation of the Th^{3+} ions, occurred during the synthesis of $Th_6F_{24} \cdot H_2O$ hydrate before the structural characterization is highlighted by these experiments.

Taking into account these results, lithium ions can diffuse within the opened channels of the structure as in an insertion compound, when the thorium ions are either oxidized ($H_2O \rightarrow Li^+$ exchange) or reduced (insertion of Li^+); we will consider the electrochemical insertion, which could induce the change of the thorium oxidation state, and the proofs of this process by ^{7}Li NMR and electron paramagnetic resonance (EPR).
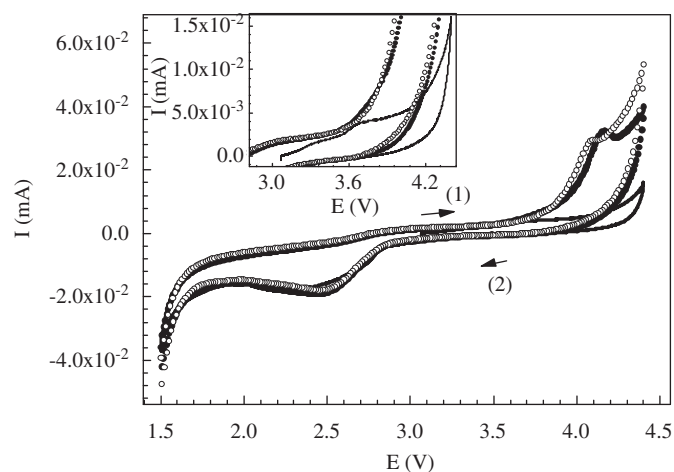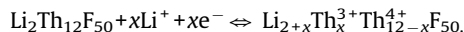

Fig. 3. 1th (straight line), 2nd (●), and 5th (○) cyclic voltamperograms of the phase $Li_{2+x}Th_{12}F_{50}$ at 60 °C.

3.2. Electrochemical insertion

$Li_{2+x}Th_{12}F_{50}$ compound was studied using cyclic voltammetry to investigate the Li^+ insertion–extraction processes according to the following equation

$$Li_2Th_{12}F_{50} + xLi^+ + xe^- \Leftrightarrow Li_{2+x}Th_x^{3+}Th_{12-x}^{4+}F_{50}.$$

The presence of anodic and cathodic peaks on the cyclic voltammetry highlights that insertion and extraction of lithium ions into the host matrix can be electrochemically performed. During the first cycle, the cycling started with the oxidation (extraction) process. Only a broad anodic wave is observed at 3.7 V (see insert in Fig. 3); its low intensity indicates that either only a few Li^+ ions can be extracted from the host matrix or the lithium content is low into the channels. In the following reduction step,

the measured cathodic peak intensity is high; the reduction of Th^{4+} ions into Th^{3+}, and the corresponding insertion of Li^+ ions into the opened channels, occur around 2.5 V. Because large amount of Li^+ ions are inserted, their extraction results in a significant anodic current. The oxidation peak is then observed at 4.2 V during the second cycle and its intensity is significantly higher than in the first cycle. This underlines that the insertion at 2.5 V and the extraction at 4.2 V are correlated. As the insertion–extraction is then initiated, the electrochemical processes are reversible, the cathodic peaks are superimposed upon cycling (see the fifth cycle in Fig. 3). On the contrary, the extraction potential slightly decreases upon cycling from 4.2 to 4.1 V. The operating temperature of 60 °C favours the reversibility upon cycling.

EPR allows the coexistence of the two oxidation states in the mixed-valence fluoride to be evidenced (Fig. 4).

First of all, the EPR spectrum at room temperature of the as-synthesized $Li_{2+x}Th_{12}F_{50}$ fluoride (Fig. 4), confirms directly the presence of Th^{3+} with $(6d)^1$ valence shell. The signal is broad and slightly anisotropic (the linewidth ΔH_{pp} was found equal to 770 ± 50 G). The value of the g-factor is equal to 2.65 ± 0.05; this large g-value may reflect the magnetic exchange between thorium ions. Diamagnetic Th^{4+} ions $(6d)^0$ act in the dilution of Th^{3+} paramagnetic ions. As a matter of fact, in the description of the structure for $Li_{5.5}M_{12}F_{50}$, two types of slabs coexist: compact slabs, which are composed of tetravalent M^{4+} cations only and opened slabs. These ones are composed with the mixed-valence ions with long range ordering of M^{3+} and M^{4+}. The Th^{3+}/Th^{4+} ratio acts on the g-factor, but also on the signal linewidth. ΔH_{PP} for the as-synthesized sample is equal to 770 ± 50 G at room temperature. When the reduction process is stopped at 1.5 V, the resulting inserted sample exhibits a signal much more intense than the initial fluoride (Fig. 4) in accordance with the increase of the Th^{3+} ion concentration. Moreover the linewidth increases for the reduced fluoride and reaches the value of 1450 ± 50 G. When the active material was electrochemically modified by an insertion of Li^+ ions, the concentration of Th^{3+} increases resulting in the reinforcement of the dipolar broadening. It must be noted that the hypothesis of the presence of paramagnetic impurities was not retained, because such defects do not depend on the lithium insertion. The increase of the EPR spin density after the electrochemical insertion cannot be explained by such kind of impurities.

3.3. Discussion

In agreement with the structure description of the $Li_{5.5}M_{12}F_{50}$ fluoride, which involves two types of lithium ions, i.e. one part locked and the other part mobile along the channel network. The reduction of M^{4+} into M^{3+} and the concomitant insertion of Li^+ into the channels result in the presence of two lines on the ^7Li NMR spectrum of the $Li_{5.5}Ce_{12}F_{50}$ fluoride [18]. The presence of Ce^{3+} paramagnetic ions in the neighbouring of Li^+ located in the channels probably allows the significant separation of the NMR lines at 0 and 21.1 ppm, assigned to locked Li^+ (denoted S_1) and mobile along the channels (S_2), respectively. This separation is less important in the ^7Li NMR spectrum of the as-synthesized $Li_{2+x}Th_{12}F_{50}$ fluoride (Figs. 2a and 5). On the contrary, when the amounts of Li^+ inserted in the channels and Th^{3+} are increased through the electroreduction, two lines are clearly observed at 0 and 5.6 ppm. The paramagnetic shift depends on the content of Th^{3+} and Li^+ ions; the higher this content is the higher the shift (i.e. 1.1 and 5.6 ppm for as-synthesized and inserted samples).
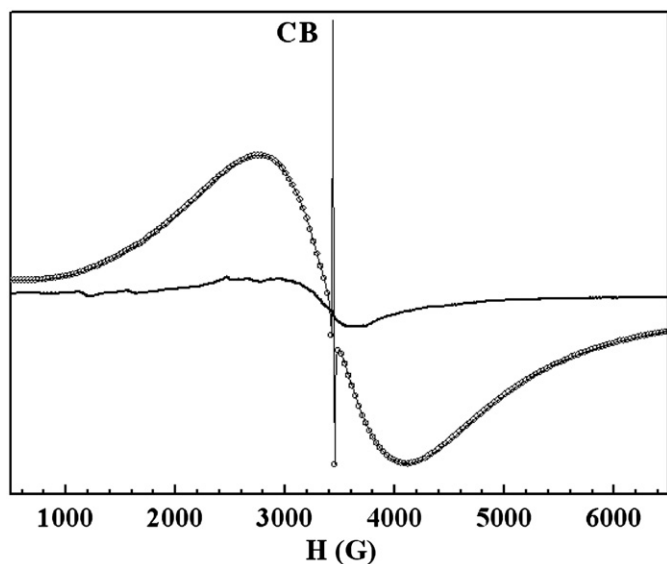

Fig. 4. An EPR spectra recorded at room temperature of the as-synthesized $Li_{2+x}Th_{12}F_{50}$ (straight line) and after reduction until 1.5 V (○). The narrow line is assigned to the carbon black used in the composite electrode ($\Delta H_{PP}=10.0 \pm 0.2$ G; $g=2.003 \pm 0.001$).
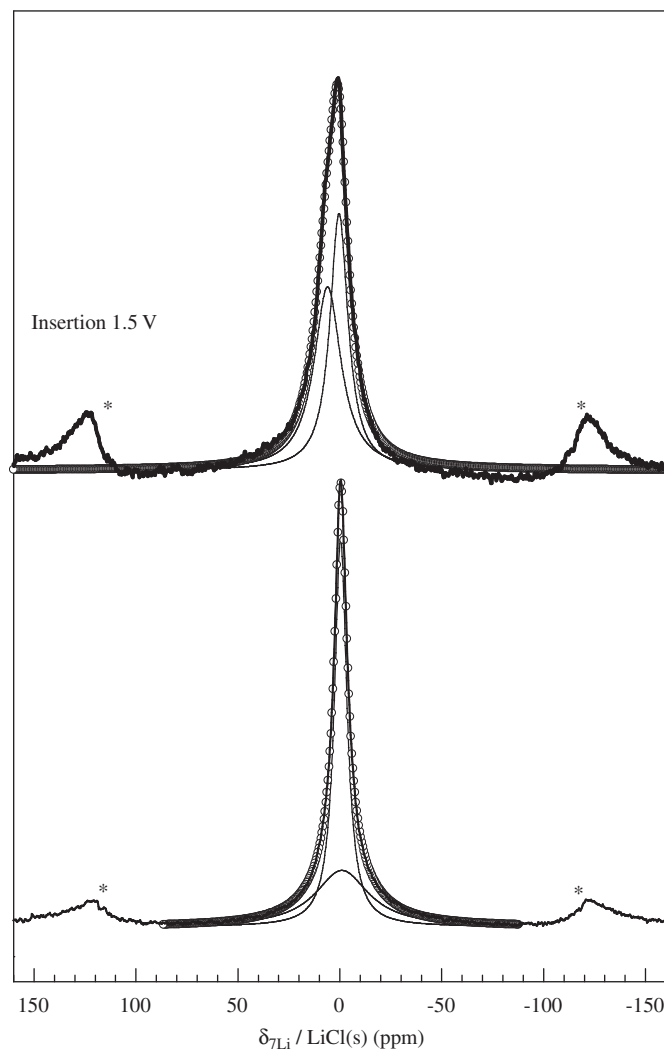

Fig. 5. An ^7Li NMR spectra (straight line) and fitting (○) using two lorentzian lines of the as-synthesized $Li_{1+x}Th_{12}F_{50}$ and the sample resulting from the electrochemical insertion. * Marks spinning sidebands.

Moreover because of the presence of Th^{3+} paramagnetic ions, the linewidth of the S_1 line is affected in comparison with the S_2 line; FWHM are equal to 1218 Hz (2220 Hz *for* $Li_{5.5}Ce_{12}F_{50}$) and 2320 Hz (3170 Hz *for* $Li_{5.5}Ce_{12}F_{50}$) for S_1 and S_2, respectively. Considering two Lorentzian lines for the fitting, the S_1/S_2 ratio of the integrated surfaces is equal to 1.1 for inserted $Li_{2+x}Th_{12}F_{50}$. Of about 0.63 and 0.69 were found for S_1/S_2 in the cases of the as-synthesized compounds, $Li_{5.5}Th_{12}F_{50}$ and $Li_{5.5}Ce_{12}F_{50}$, respectively. Taking into account the crystal structure, the S_1/S_2 theoretical ratio should be equal to 2/3.5 i.e. 0.57 [18]. As reported for the cerium mixed-valence, because of the opened structure of $Li_{5.5}M_{12}F_{50}$ fluoride, the insertion compound can exhibit large change in the stoichiometry, better formulated $Li_{2+x}Ce_x^{3+}Ce_{12-x}^{4+}F_{50}$. The increase of the S_1/S_2, resulting from the electrochemical insertion of Li^+ ions, underlines that the Th^{3+}/Th^{4+} ratio was significantly increased.

From NMR data, the S_1/S_2 ratio is related to the ratio of the amount of Li^+ in the locked position and in the channels. As $S_1/S_2=1.1$ and the number locked Li^+ ions is equal to 2 per $Li_{2+x}Th_x^{3+}Th_{12-x}^{4+}F_{50}$ formulae unit (extracted from the XRD structure), 1.82 Li^+ ions are located in the channels. The stoichiometry seen by ^7Li NMR is $Li_{2+1.82}Th_{1.82}^{3+}Th_{10.18}^{4+}F_{50}$. Similar calculations can be done with the amount of inserted or extracted Li^+ ions (N_{Li+}) taking into account the current intensity and time, *i.e.* related to the area of the anodic or cathodic peak of the voltammogram (Fig. 3). The number of Li^+ ions, N_{Li+}, is estimated of 1.77 and 1.35 Li^+ ions per $Li_{2+x}Th_{12}F_{50}$ formula unit during the fifth insertion and extraction processes, respectively. For the comparison with the value as seen by ^7Li NMR for the sample obtained after an electroreduction until 1.5 V, the value during the insertion process is considered and the estimated stoichiometry is $Li_{2+1.77}Th_{1.77}^{3+}Th_{10.23}^{4+}F_{50}$. A good agreement between the two methods is found and the stoichiometry of the inserted compound close to $Li_{3.8}Th_{1.8}^{3+}Th_{10.2}^{4+}F_{50}$ can be proposed.

Several mixed-valence terbium fluorides were investigated such as Tb_4F_{15} compound [12,13], potassium containing terbium fluorides $K_2Tb_4F_{17}$ and KTb_3F_{12} [14,15], and also aluminum containing terbium fluorides $Rb_2AlTb_3F_{16}$ [16] and $RbAl_2Tb_4F_{22}$ [17]. In a general way, the synthesis of mixed-valence compounds depends on the reaction atmosphere, reducing or oxidizing, but the case of M^{3+}/M^{4+} mixed-valence fluorides (M corresponds to lanthanide or actinide element) is particular and the processes are controlled by the decomposition temperature of the "free" MF_4 tetrafluoride. For instance, the analysis of KF–TbF_3–TbF_4 ternary system and the corresponding three binary systems allows to better understand the conditions of appearance of the mixed-valence in the terbium fluorides. Any compound with KF/TbF_4 ratio higher than 1, *i.e.* $KTbF_5$, was highlighted in the KF–TbF_4 binary system (including K_3TbF_7, K_2TbF_6, $K_7Tb_6F_{31}$ and $KTbF_5$). Indeed, by the constraint for +4 terbium ions to be obligatorily in eight coordination in fluorinated environment [6–11], the combinations with potassium fluoride are limited. This obligation does not exist for Tb^{3+} and a series of trivalent terbium fluorides covers all the composition range K_3TbF_6–KTb_3F_{10} (the intermediate fluorides are K_2TbF_5, $KTbF_4$, and KTb_2F_7). In KF–TbF_4 binary system, an enrichment of the reactive mixture above the limit of the TbF_4/KF molar ratio equal to 1 results in an excess of tetravalent element. However this terbium tetrafluoride excess, non-associated with KF in a defined tetrafluoride compound, thermally behaves like "free" TbF_4. Chilingarov et al. [25] showed that the decomposition of TbF_4 into TbF_3 and atomic fluorine occurs at temperatures higher than 550 °C even in fluorine atmosphere. If the synthesis conditions allow it, TbF_4 in excess releases by decomposition trivalent fluoride, which is suitable to immediately combine with the other components of the reactive mixture. This forms Tb^{3+}/Tb^{4+} mixed-valence terbium fluoride. In other words, an induced transformation occurs during the thermal treatment from the KF–TbF_4 binary into KF–TbF_3–TbF_4 ternary system. The obtained mixed-valence compounds are thermodynamically stable. Thus, the terbium fluorides initially formulated

KTb_2F_9 ($TbF_4/KF=2$) is actually a mixed-valence compound with $K_2Tb_4F_{17}$ formula, i.e. $K_2Tb^{III}Tb_3^{IV}F_{17}$ [10,11]. Moreover it is to note that the presence of alkaline fluorides or other elements such as aluminum fluoride modifies the temperature of TbF_4 into TbF_3 conversion and this seems to favour the mixed-valence, in particular KF, RbF, and CsF for the case of terbium fluoride. These observations about terbium fluorides are useful to understand the appearance of mixed-valence in actinide and lanthanide fluorides. By analogy with terbium tetrafluorides, the presence of lithium ions may favour the mixed-valence in thorium fluoride and Th^{3+} may be formed *in situ* by decomposition of the "free" ThF_4. The presence of Th^{3+} ions instead of Th^{4+} needs the compensation of the decrease of the positive charge. The vacancies of F^- has been first investigated, because it could result in an EPR response as hole center. Nevertheless, such hypothesis cannot explain the changes after the electrochemical insertion. As a matter of fact, under our conditions, i.e. with an $LiClO_4/PC$ electrolyte, Li^+ ions can be reversibly exchanged contrary to F^-. On the contrary, the insertion of lithium ions into the opened channels of the structure results in the compensation of anionic and cationic charges. Each time that a Th^{4+} ion is replaced by Th^{3+}, one additional Li^+ ion is inserted into the channel. This process is reversible and does not change significantly the crystal structure. The existence of the opened channel has been proved with the cerium mixed-valence $Li_{5.5}Ce_{12}F_{50}$, which is unambiguously isostructural with the present compound. Moreover the possible diffusion of Li^+ ions along the channel has been proved by the exchange of these ions by water molecules.

4. Conclusion

The present work underlines the existence of Th^{3+} ions in mixed-valence fluorides and also completes the study of fluorides with general formula $Li_{2+x}M_x^{3+}M_{12-x}^{4+}F_{50}$ with M=Ce and Th. The coexistence of the M^{3+} and M^{4+} oxidation states in these compounds has been confirmed in a previous paper by XRD, XPS, and solid state NMR.

First of all, it has been shown that the thorium and cerium mixed-valence fluorides are isostrutural. Their structure exhibits an opened channels network, where a part of the lithium ions are located, the other Li^+ ions being locked. The M^{4+} into M^{3+} reduction and the concomitant insertion of Li^+ into the channel can be electrochemically performed, thanks to the liquid electrolyte. The thorium mixed-valence fluoride appears then as an insertion compound with general stoichiometry $Li_{2+x}Th_x^{3+}Th_{12-x}^{4+}F_{50}$. This thorium fluoride is very original because, on one hand, only a few actinide or lanthanide mixed-valence fluorides are reported in the literature and, on the other hand, Th^{3+} ions are very unusual in the solid state. ^1H and ^7Li solid state NMR data evidence the possible exchange between Li^+ and H_2O and explains the ambiguity about the real composition reported in the literature about thorium fluoride with Th/F atomic ratio close to 4, i.e. $LiTh_4F_{17}$ and $Th_4F_{16}\cdot H_2O$.

The electrochemical insertion–extraction process allows the control of the Th^{3+}/Th^{4+} ratio contrary to the solid state synthesis, for which the mixed-valence appearance may be related to the decomposition of "free" tetrafluoride. This decomposition depends on the extent of the tetrafluoride excess, the temperature and the cooling rate. This study suggests that the content of Li^+, and then Th^{3+}, can be increased or, on the contrary, decreased to synthesize by an original way new fluorides with variable $Li_{2+x}Th_x^{3+}Th_{12-x}^{4+}F_{50}$ composition. The changes of the Li^+ and Th^{3+} content have been followed by solid state ^7Li NMR and EPR, respectively.

Taking into account the structure, the lower limit is close to $Li_2Th_{12}F_{50}$, where $x=0$ in $Li_{2+x}Th_x^{3+}Th_{12-x}^{4+}F_{50}$. Works are in progress to investigate to upper limit. Such an electrochemical synthesis would

then be extent to other mixed-valence fluorides with similar opened structure, in particular with channels containing lithium ions.

Appendix A. Supplementary materials

Supplementary data associated with this article can be found in the online version at doi:10.1016/j.jssc.2010.10.010

References

[1] K.M. MacKay, R.A. MacKay, W. Henderson, in: Introduction to Modern Inorganic Chemistry, sixth ed., Nelson Thornes Ltd, Versita, co-published with Springer-Verlag GmbH, 2002 chap. 12, p. 263.
[2] M.S. Wickleder, B. Fourest, P.K. Dorhout, in: The Chemistry of the Actinide and Transactinide Elements, Springer, Netherlands, 2006 chapter. 3, pp. 52–160.
[3] H.J. Emeléus, Advances in Inorganic Chemistry and Radiochemistry, vol. 28, Academic press, 1984.
[4] B.B. Cunningham, D.C. fray, M.A. Rollier, J. Am. Chem. Soc. 76 (1954) 3361.
[5] R. Hoppe, K.M. Rödder, Z. Anorg. Allg. Chem. 312 (1961) 277–278.
[6] D. Avignant, J.-C. Cousseins, C.R. Acad. Sci. Paris, Ser. C 278 (9) (1974) 613–616.
[7] Y. Laligant, A. Le Bail, G. Ferey, D. Avignant, J.-C. Cousseins, Eur. J. Solid State Inorg. Chem. 25 (5–6) (1989) 551–563.
[8] D. Avignant, J.-C. Cousseins, Rev. Chim. Miner. 15 (1978) 360–367.
[9] M. El-Ghozzi, D. Avignant, J.-C. Cousseins, Eur. J. Solid State Inorg. Chem. 29 (6) (1992) 981–992.
[10] V. Gaumet, D. Avignant, Acta Crystallogr. C53 (9) (1997) 1176–1178.
[11] M. Josse, M. Dubois, M. El-Ghozzi, D. Avignant, J. Alloys Compd. 374 (1–2) (2004) 213–218.
[12] M.N. Brekhovskikh, A.I. Popov, M. Yu, A. Il'inskii, V.A. Fedorov, Russ. J. Inorg. Chem. 34 (1989) 573–577.
[13] A.I. Popov, M.D. Val'kovskii, P.P. Fedorov, M. Yu Kiselev, Russ. J Inorg. Chem. 36 (1991) 476–480.
[14] D. Avignant, E. Largeau, V. Gaumet, P. Dugnat, M. El-Ghozzi, J. Alloys Compd. 275–277 (1998) 1–5.
[15] E. Largeau, M. El-Ghozzi, D. Avignant, J. Solid State Chem. 139 (1998) 248–258.
[16] M. Josse, M. Dubois, M. El-Ghozzi, D. Avignant, Solid State Sci. 5 (2003) 1141–1148.
[17] M. Josse, M. Dubois, M. El-Ghozzi, D. Avignant, J. Alloys Compd. 374 (2004) 213–218.
[18] G. Renaudin, B. Dieudonné, E. Mapemba, M. El-Ghozzi, D. Avignant, M. Dubois, Inorg. Chem. 40 (2010) 370–375.
[19] G. Renaudin, E. Mapemba, M. El-Ghozzi, M. Dubois, D. Avignant, R. Cerny, Z. Kristallogr. 26 (2007) 455–460.
[20] R.E. Thoma, H. Insley, B.S. Pram, H.A. Friedman, W.R. Grimes, J. Phys. Chem. 63 (1959) 1267.
[21] C.J. Barton, H.A. Friedman, W.R. Grimes, H. Insley, R.E. Moore, R.E. Thoma, J. Am. Ceram. Soc. 41 (1958) 63–69.
[22] A. Cousson, Mr. Pages, J.C. Cousseins, A. Vedrine, J. Cryst. Growth 40 (1977) 157–160.
[23] A. Cousson, Mr. Pages, R. Chevalier, Acta Crystallogr. B35 (1979) 1763–1765.
[24] *FullProf.2k*—version 3.30, Rodriguez-Carvajal, J., Laboratoire Léon Brillouin (CEA-CNRS), France. (2005).
[25] N.S. Chilingarov, J.V. Rau, L.N. Sidorov, L. Bencze, A. Popovic, V.F. Sukhoverkhov J. Fluorine Chem. 104 (2000) 291-295.